Organic & Biomolecular Chemistry

This article is part of the

OBC 10th anniversary

themed issue

All articles in this issue will be gathered together online at

www.rsc.org/OBC10

Organic & Biomolecular Chemistry

Dynamic Article Links
View Online

Cite this: *Org. Biomol. Chem.*, 2012, **10**, 5985

www.rsc.org/obc

PAPER

Construction of multi-component supramolecular architectures of bile acids and cinchona alkaloids through helical-pitch-synchronized crystallization†

Toshiyuki Sasaki, Norie Shizuki, Eri Hiraishi, Ichiro Hisaki,* Norimitsu Tohnai and Mikiji Miyata*

Received 11th January 2012, Accepted 15th March 2012
DOI: 10.1039/c2ob25072a

Molecular assemblies based on helical motifs are of substantial interest from the view point of fundamental science as well as application. In this study, we propose a new class of organic crystal, that is, heteroH-MOC (multi-component organic crystal containing different kinds of helical motifs consisted of different components), and describe successful construction of heteroH-MOCs with $P2_1$ and $P2_12_12_1$ space groups by using steroidal bile acids and cinchona alkaloids. In the $P2_1$ crystals, two kinds of helices composed of the steroid and alkaloid are arranged in a parallel fashion, while, in the $P2_12_12_1$ crystals, those are in a perpendicular fashion. It is remarkable that, in such systems, particularly in the latter crystals, components ingeniously achieved highly-ordered synchronization of periodicity (helical pitches *r* and periodic distances in the array of helices *p*), which is first demonstrated in this study through hierarchical interpretation of the crystal structures.

Introduction

Helices are one of the most sophisticated and fascinating highly-ordered structures which nature has selected to exhibit significant biological and physical functionalities. Inspired by naturally-occurring exotic helical structures such as the DNA double helix, to date a number of helical structures have been achieved in various scales and phases.[1–5] Furthermore, well-controlled supramolecular arrangements based on helices have recently been reported. For example, Yashima and co-workers revealed arrangements and chirality of helical poly(phenylacetylene) derivatives or stereocomplexes of poly(methyl methacrylate)s laid on highly oriented pyrolytic graphite (HOPG) by atomic force microscopy (AFM).[6] Shinkai and co-workers constructed and controlled supramolecular arrangements of carbon nanotubes wrapped by helical polymers of modified β-1,3-glucans.[7] Construction of helical structures in organic crystals has also been intensively investigated because of the following three aspects. (1) Organic crystals can achieve Avogadro's numbers of helical assemblies arranged with extreme regularity, enabling exhibition of highly anisotropic physical properties. (2) X-Ray crystallographic analysis using single crystals can reveal complicated helical architectures which are difficult to characterize spectroscopically. (3) Organic molecules particularly prefer to crystallize with two-fold (2_1) helical symmetry,[8] which is observed for *ca.* 70% of crystals registered in the Cambridge Structural Database (CSD).[9]

To achieve complicated helical supramolecular architectures in the crystalline state, multi-component organic crystals (MOCs) are one of the potential systems.[10,11] Particularly, combination of acidic and basic components is often applied because salt-bridge or charge-assisted hydrogen bonds can easily connect different components and prevent segregated crystallization of the respective components (Fig. 1a). Furthermore, high-throughput co-crystallization by combining one component with various other components can be easily carried out to construct desired helical structures. To date, MOCs containing the same kinds of helical motifs (homoH-MOCs) (Fig. 1b) have been reported to exhibit significant properties such as nonlinear optical properties[12] and chiral discrimination abilities.[13] However, MOCs composed of different kinds of helical motifs of different components (heteroH-MOCs) as shown in Fig. 1c still remain challenging targets.

For construction of heteroH-MOCs, the components have a need to satisfy periodic requirements in addition to salt-bridged-complexation of components.[14] For example, a crystal with the space group of $P2_1$ shown in Fig. 1c (left) should synchronize pitches of helical motifs along the *b* axis and periodic distances of helices along the *a* axis ($r_A = r_B$, and $p_A = p_B$, respectively, where r_A and r_B denote helical pitches of acidic and basic components, respectively, while p_A and p_B do periodic distances in arrays of acidic and basic helices, respectively). Furthermore, a $P2_12_12_1$ crystal should achieve synchronization between helical pitch and periodic distance of helices ($r_A = p_B$ and $r_B = p_A$) along the *a* and *b* axes, respectively, as shown Fig. 1c (right).

2-1 Yamadaoka, Suita, Osaka 565-0871, Japan. E-mail: hisaki@mls.eng.osaka-u.ac.jp, miyata@mls.eng.osaka-u.ac.jp; Fax: +81-6-6879-7404; Tel: +81-6-6879-7404

†CCDC 862701–862705 for **1a·3a**H, **1b·3a**H, **1d·4a**H, **1e·3a**H and **1e·3b**H. For crystallographic data in CIF or other electronic format see DOI: 10.1039/c2ob25072a.

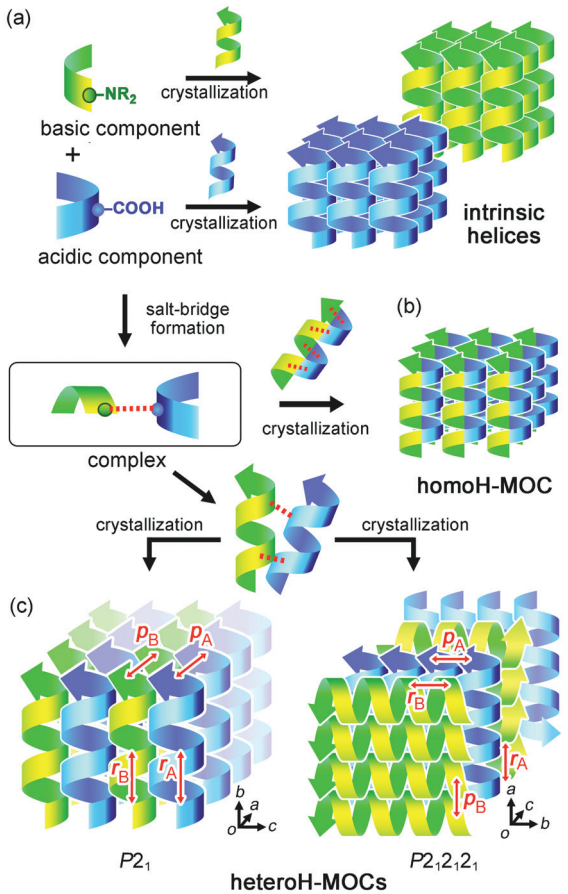

Fig. 1 Schematic representation of crystals with helical motifs: (a) mono-component crystals with intrinsic helical motifs, (b) homoH-MOC formed *via* a salt-bridged complex of basic (green) and acid (blue) components, (c) heteroH-MOCs with the space groups of $P2_1$ (left) and $P2_12_12_1$ (right) formed *via* a salt-bridged complex of basic (green) and acidic (blue) components. In the heteroH-MOCs, two kinds of helical motifs periodically synchronized each other: $r_A = r_B$ and $p_A = p_B$ for the $P2_1$ crystal, $r_A = p_B$ and $r_B = p_A$ for the $P2_12_12_1$ crystal, where r_A and r_B denote helical pitches of acidic and basic components, respectively, while p_A and p_B do periodic distances in arrays of acidic and basic helices, respectively. The salt-bridge is drawn by red dash line. Handedness of helices is drawn arbitrarily.

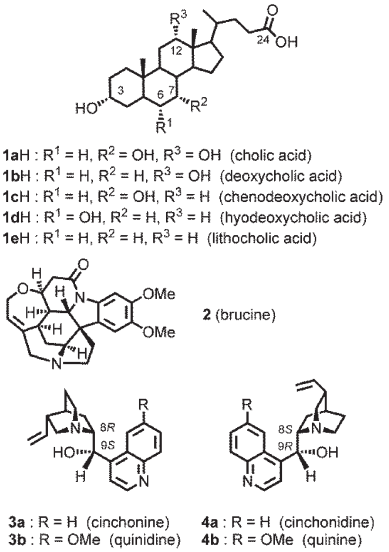

Scheme 1 Naturally-occurring asymmetric compounds as building blocks of heteroH-MOCs.

Table 1 Co-crystallization of bile acids and cinchona alkaloids[a,b,c]

	3a	3b	4a	4b
1aH	**1a**·**3a**H ($P2_12_12_1$)	—	—	—
1bH	**1b**·**3a**H ($P2_12_12_1$)	—	—	—
1cH	—	—	—	—
1dH	—	—	**1d**·**4a**H ($P2_1$)	–
1eH	**1e**·**3a**H ($P2_1$)	**1e**·**3b**H ($P2_1$)	—	—

[a] **1a**·**3a**H, **1b**·**3a**H, **1e**·**3a**H, **1e**·**3b**H, and **1d**·**4a**H denote heteroH-MOCs composed of carboxylate (**1a**$^-$, **1b**$^-$, **1d**$^-$, or **1e**$^-$) and ammonium (**3a**H$^+$, **3b**H$^+$, or **4a**H$^+$) components, while bars (—) denote amorphous materials. [b] The space groups of the obtained crystals are in the parentheses. [c] Bile acid and cinchona alkaloid were mixed with 1 : 1 molar ratio to obtain a salt. Recrystallization of the salt was performed with THF or 1,4-dioxane at ambient temperature.

In connection with this, we recently reported construction of a heteroH-MOC with the space group of $P2_1$ composed of naturally-occurring polycyclic compounds, cholic acid **1a**H and brucine **2**.[15] In the crystal, **1a**$^-$ and **2**H$^+$ respectively formed 2_1 symmetric helical assemblies and the assemblies were arranged in a parallel fashion. It was important that the helices of **1a**$^-$ and **2**H$^+$ synchronized their pitches with each other to establish three dimensional crystal structures.[15]

In this paper, we first report construction of heteroH-MOCs composed of 2_1 helices of bile acids and cinchona alkaloids (Scheme 1), in which two kinds of arrangements of helical motifs were achieved, that is, the parallel- and perpendicular arrangements to give crystals with space groups of $P2_1$ and $P2_12_12_1$, respectively. We performed hierarchical interpretation[16] of the crystals and demonstrated ingenious periodic synchronization of the helical motifs achieved in the crystals. Furthermore, heteroH-MOCs of **1d**·**4a**H, **1e**·**3a**H and **1e**·**3b**H have significantly asymmetric inclusion channels surrounded by two different helical structures.

Results and discussion

To construct heteroH-MOCs composed of a bile acid and cinchona alkaloid, co-crystallization was performed through screening experiments with five bile acids possessing different numbered and positioned hydroxyl groups and four cinchona alkaloids (Scheme 1). Since design of crystal structures composed of such complex and asymmetric molecules is still significantly difficult, trial-and-error crystallization with a screen method is an effective way to obtain the desired structures. The results of crystallization are shown in Table 1. Interestingly, formation of single crystals was strongly dependent on the derivatives used. Namely, **3a** gave crystals of complexes with **1a**H, **1b**H, and **1e**H, while its

pseudo-enantiomer **4a** did with only **1d**H. Alkaloid **3b** co-crystallized only with **1e**H, while **4b** gave no crystal with any bile acids. These results imply the following three points. (1) The number and position of the hydroxyl groups in the bile acids critically affects on lattice type of crystals. (2) The methoxy group in the quinoline rings of **3b** and **4b** would work unfavorably for co-crystallization with steroids due to its steric repulsion. (3) Absolute configuration of (*S*, *R*) at the C8 and C9 carbon atoms of the alkaloids would be preferable, which is often observed in diastereomeric salt formation for optical resolution. Detailed structures of the obtained crystals are described below.

Construction of monoclinic heteroH-MOCs with the $P2_1$ space group, 1e·3aH and 1e·3bH

Bile acid **1e**H with **3a** or **3b** formed a salt **1e**$^-$·**3a**H$^+$ or **1e**$^-$·**3b**H$^+$ and co-crystallized into the monoclinic space group of $P2_1$ (**1e·3a**H or **1e·3b**H, respectively). Fig. 2a shows a packing diagram of **1e·3a**H viewed down from the *b* axis. The crystal **1e·3a**H has a heteroH-MOC structure in which two different 2_1 helices are arranged in a parallel fashion. Lithocholate **1e**$^-$ forms a rhombic-shaped 2_1 helical assembly along the *b* axis through multiple hydrogen bonds involving hydroxyl groups at the 3-position and the carboxylate, as well as a water molecule: O3–H···O24*A* and O24···H–O3*B* (O···O distance: 2.643 Å), O3···H–O_{w1}*B* (O···O distance: 2.733 Å), and O′24···H–O_{w1} (O···O distance: 2.687 Å), as shown in Fig. 2b. The present assembly pattern of **1e**$^-$ is different from that reported in the literature.[17] The motifs are stacked with adjacent ones along the *a* axis with their lipophilic β-faces contacting each other through van der Waals interactions. Cinchonium **3a**H$^+$ also forms 2_1 helical assembly through water-intermediated intermolecular hydrogen bonding networks (O_{3a}···H–O_{w2}–H···N_{3a}2*A*, O_{3a}*B*···H–O_{w2}*B*–H···N_{3a}2, O···O distance: 2.912 Å, O···N distance: 2.890 Å) and edge-to-face (CH/π) interactions between the neighbouring quinoline rings (dihedral angle of the quinoline rings: 38.9°), as shown in Fig. 2c. The assemblies of **1e**$^-$ and **3a**H$^+$ can be described as right-handed helices on the basis of supramolecular tilt chirality, as shown Fig. 3,[16b,18,19] where the directions of the arrows in the helical models of **1e**$^-$ and **3a**H$^+$ correspond to that from the tail to head of **1e**$^-$ components and that from the concave to convex ends in the herringbone assembly of **3a**H$^+$. The components **1e**$^-$ and **3a**H$^+$ are linked by a salt-bridge (O′24···H–N_{3a}1 with O···N distance of 2.65 Å) as shown in Fig. 2d.

Consequently, construction of the heteroH-MOCs **1e·3a**H can be described by a hierarchical scenario as shown in Fig. 4, which experiences (i) formation of hetero helices connected by the salt-bridge, (ii) layer formation by translational assembly of the helices, and (iii) lamination of the layer accompanied by guest inclusion into the void space. In the crystal, the helical motifs achieved periodic synchronization with the unique pitch of $r_A = r_B = 7.89$ Å and periodic distance for arrays of acidic and basic helices of $p_A = p_B = 11.41$ Å.

It is noteworthy that the crystal has infinite inclusion channels accommodating a recrystallization solvent 1,4-dioxane along the

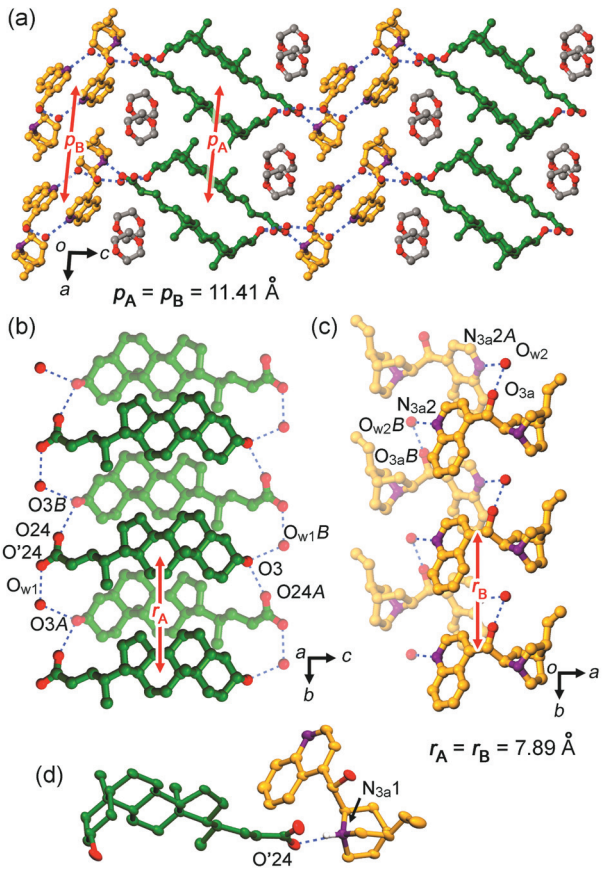

Fig. 2 Crystal structure of **1e·3a**H. (a) Packing diagram. (b, c) 2_1 Helical motifs of **1e**$^-$ and **3a**H$^+$, respectively. (d) Salt-bridge between **1e**$^-$ and **3a**H$^+$. Carbon atoms of **1e**$^-$, **3a**H$^+$, and dioxane were coloured by green, orange, and gray, respectively, while oxygen and nitrogen atoms by red and purple, respectively. All hydrogen atoms except for that in the salt bridge were omitted for clarity. Symmetry code: for (b) (*A*) $1 - x$, $1/2 + y$, $1 - z$; (*B*) $1 - x$, $-1/2 + y$, $1 - z$; for (c) (*A*) $1 - x$, $-1/2 + y$, $-z$; (*B*) $1 - x$, $1/2 + y$, $-z$.

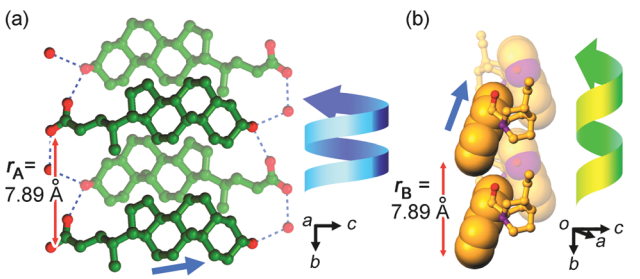

Fig. 3 Determination of helical handedness for 2_1 helices of **1e**$^-$ and **3a**H$^+$. (a) Right-handed 2_1 helix of **1e**$^-$, whose handedness was determined on the basis of the tilt of the steroidal skeleton. (b) Right-handed 2_1 helix of **3a**H$^+$, whose handedness was determined on the basis of the tilt of the quinoline rings drawn with the space fill model. Carbon atoms of **1e**$^-$ and **3a**H$^+$ were coloured by green and orange, respectively, while oxygen and nitrogen atoms by red and purple, respectively. The direction of the arrow in the helical model of **1e**$^-$ corresponds to that from the tail to head of **1e**$^-$. The direction of the arrow in the helical model **3a**H$^+$ corresponds to that from concave to convex ends in the herringbone assembly of **3a**H$^+$. All hydrogen atoms were omitted for clarity. Symmetry code: (*A*) $1 - x$, $1/2 + y$, $1 - z$; (*B*) $1 - x$, $-1/2 + y$, $1 - z$.

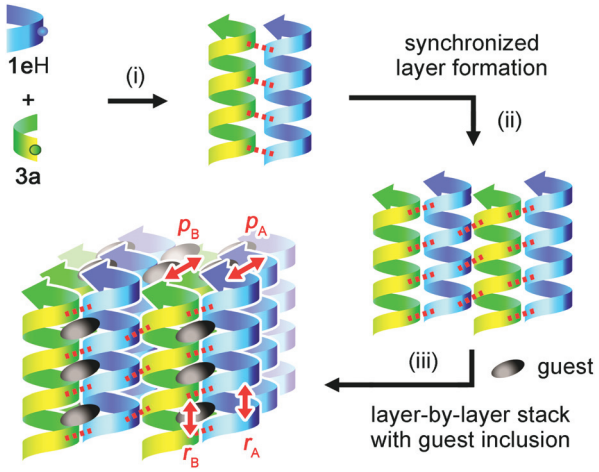

Fig. 4 Schematic representation for a hierarchical scenario to construct heteroH-MOC **1e·3a**H. The scenario contains the following processes: (i) formation of hetero helices by connection of right helices through the salt bridge, (ii) layer formation, and (iii) lamination of the layer accompanied by guest inclusion into the void space. The periodic synchronization: $r_A = r_B = 7.89$ Å and $p_A = p_B = 11.41$ Å.

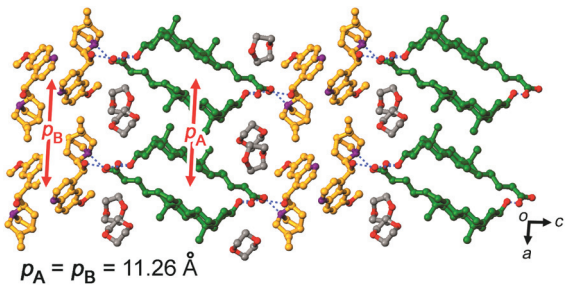

Fig. 5 Packing diagram of **1e·3b**H. Carbon atoms of **1e**$^-$, **3b**H$^+$, and dioxane were coloured by green, orange, and gray, respectively, while oxygen and nitrogen atoms by red and purple, respectively. All hydrogen atoms were omitted for clarity.

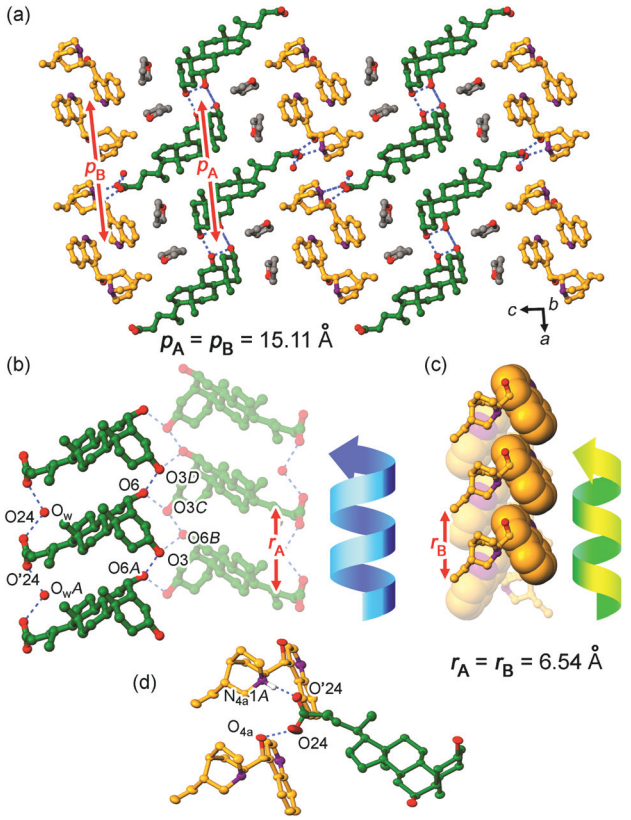

Fig. 6 Crystal structure of **1d·4a**H. (a) Packing diagram viewed down from the *b* axis. (b) Right-handed 2_1 helical motif of **1d**$^-$. (c) Left-handed 2_1 helical motif of **4a**H$^+$, where the quinoline rings of **4a**H$^+$ are drawn with the space fill model. (d) Salt-bridge between **1d**$^-$ and **4a**H$^+$. Carbon atoms of **1d**$^-$, **4a**H$^+$, and THF were coloured by green, orange, and gray, respectively, while oxygen and nitrogen atoms by red and purple, respectively. All hydrogen atoms except for that in the salt bridge were omitted for clarity. Symmetry code: for (b) (*A*) $x, -1 + y, z$; (*B*) $1 - x, -1/2 + y, 1 - z$; (*C*) $1 - x, 1/2 + y, 1 - z$; (*D*) $x, 1 + y, z$; for (d) $x, -1 + y, z$.

b axis. Conventionally, many of bile acid derivatives gave 2_1 symmetrical inclusion channels. The crystal **1e·3a**H, however, gave the channels with much lower symmetry because the walls of the channel are surrounded by aliphatic moieties of **1e**$^-$ and quinoline moiety of **3a**H$^+$.

Combination of **1e**H and **3b** also gave monoclinic crystal **1e·3b**H with the $P2_1$ space group, whose framework is quite similar with that of **1e·3a**H (Fig. 5). The crystal, however, is not frequently obtained and its quality is relatively low compared with that of **1e·3a**H: The 1,4-dioxane molecules accommodated in the inclusion channel are significantly disordered, and thus were resolved isotropically. This result indicates that the methoxy group of the quinoline ring hinders construction of the framework.

Construction of monoclinic heteroH-MOC with the $P2_1$ space group, 1d·4aH

Compounds **1d**H and **4a** co-crystallized into the monoclinic space group of $P2_1$ with including THF and water molecules. The obtained crystal was too small for crystallographic analysis by a general diffraction apparatus. Therefore, the crystal was subjected to synchrotron X-ray diffraction analysis, revealing its crystal structure although its quality is still unsatisfactory. As shown in Fig. 6, **1d**$^-$ and **4a**H$^+$ formed respective 2_1 helical motifs along the *b* axis (Fig. 6a). Components **1d**$^-$ are connected through two hydrogen bonding networks: O3–H···O6*B*–H···O3*C* (O3···O6*B*: 2.826 Å, O6*B*···O3*C*: 2.870 Å) and O_wA–H···O′24–C–O24···H–O_w (O_w···O′24: 2.729 Å, O24···O_w: 2.669 Å) to give right-handed helix, where the direction of the arrow in the helical model of **1d**$^-$ corresponds to that from the tail to head of the steroidal skeleton of **1d**$^-$ (Fig. 6b). The helical motif of **1d**$^-$ is similar with that reported in the literature.[20] Cinchonidium **4a**H$^+$ formed a herringbone type left-handed 2_1 helical assembly through CH/π interactions between the quinoline rings, where the direction of the arrow in the helical model of **4a**H$^+$ corresponds to that from the concave to convex ends in the herringbone assembly of **4a**H$^+$ (Fig. 6c). Components **1d**$^-$ and **4a**H$^+$ are connected through the salt-bridge ($N_{4a}1A$–H···O′24, N···O distance: 2.665 Å) and hydrogen bond (O_{4a}–H···O24, O···O distance: 2.595 Å) (Fig. 6d). The framework also has

asymmetric one-dimensional inclusion channels accommodating THF molecules.

Construction of the heteroH-MOCs **1d·4a**H can also be described by a hierarchical scenario as shown in Fig. 7, which experiences (i) formation of hetero helices by connection of right- and left-handed helices through the salt-bridge, (ii) layer formation, and (iii) lamination of the layer accompanied by guest inclusion into the void space. In the crystal, the helical motifs achieved periodic synchronization with pitches of $r_A = r_B =$ 6.54 Å, and periodic distances for arrays of acidic and basic helices of $p_A = p_B =$ 15.11 Å. The helical pitch of **1d·4a**H ($r_A = r_B =$ 6.54) is shorter than that of the pseudo-diastereomeric crystal **1e·3a**H ($r_A = r_B =$ 7.89). This difference attributes from the dihedral angles of the adjacent quinoline rings: 61.1° for **1d·4a**H and 38.9° for **1e·3a**H.

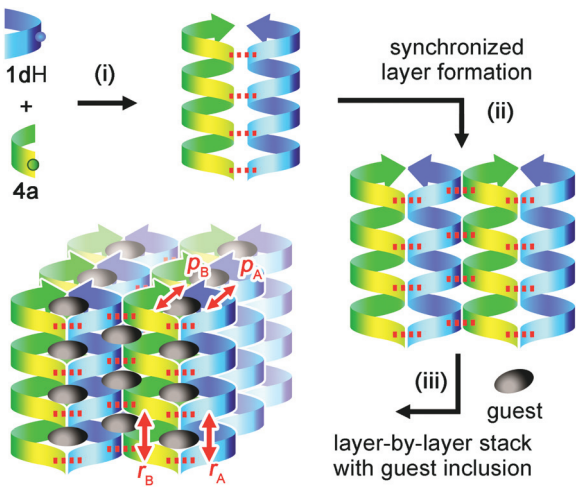

Fig. 7 Schematic representation for a hierarchical scenario to construct heteroH-MOC **1d·4a**H. The scenario contains the following processes: (i) formation of hetero helices by connection of right- and left-handed helices through the salt bridge, (ii) layer formation, and (iii) lamination of the layer accompanied by guest inclusion into the void space. The periodic synchronization: $r_A = r_B =$ 6.54 Å and $p_A = p_B =$ 15.11 Å.

Construction of orthorhombic heteroH-MOCs with the $P2_12_12_1$ space group, 1a·3aH and 1b·3aH

Compounds **1a**H with **3a** co-crystallized into $P2_12_12_1$ space group, in contrast with the former three crystals. Fig. 8a shows the packing diagram of **1a·3a**H viewed down from the *a* axis. Layers composed of $\mathbf{1a}^-$ and $\mathbf{3aH}^+$ (Fig. 8c,e) laminate alternately along the *c* axis. In each layer, the component, $\mathbf{1a}^-$ or $\mathbf{3aH}^+$, forms a hydrogen bonded 2_1 helical motif, which then aligns in parallel manner to construct the layer. As shown in Fig. 8f, $\mathbf{3aH}^+$ makes hydrogen bonds ($O_{3a}A$–H···$N_{3a}2$ and O_{3a}–H···$N_{3a}2B$, O···N distance: 2.614 Å) to form the helical assembly which is a typical motif for salts and solvates of cinchona alkaloids.[21] On the other hand, it is noteworthy that $\mathbf{1a}^-$ gave a new helical motif completely different from those ever reported.[22,23] For example, in the heteroH-MOC of **1a·2**H that we previously reported,[15] $\mathbf{1a}^-$ kept its intrinsic 2_1 helical motif. In the present system, however, $\mathbf{1a}^-$ altered its helical motif flexibly. As shown in Fig. 8d, $\mathbf{1a}^-$ is arranged into a herringbone fashion through multiple hydrogen bonds: O7–H···O3*B* and O3–H···O7*A* with O···O distance of 2.933 Å and O12–H···O3*B* and O3–H···O12*A* with O···O distance of 2.796 Å. The motif is then connected to the neighbor one through hydrogen bond O24···H–O12 with O···O distance of 2.652 Å. The motifs of $\mathbf{1a}^-$ and $\mathbf{3aH}^+$ can be described as left- and right-handed helices, respectively, on the basis of supramolecular tilt chirality,[18] where the direction of the arrow in the helical model of $\mathbf{1a}^-$ corresponds to that from the tail to head of the steroidal skeleton of $\mathbf{1d}^-$, while

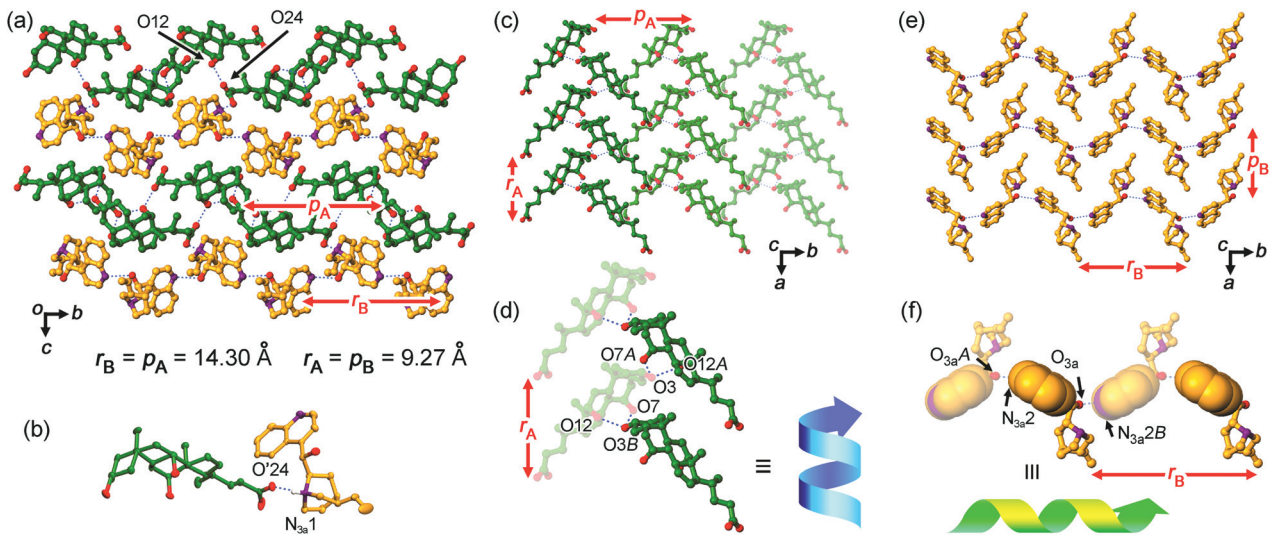

Fig. 8 Crystal structure of **1a·3a**H. (a) Packing diagram viewed down from the *a* axis. (b) Salt-bridge formed between $\mathbf{1a}^-$ and $\mathbf{3aH}^+$. (c, e) Sheet structures of $\mathbf{1a}^-$ and $\mathbf{3aH}^+$, respectively. (d, f) 2_1 Helical motifs of $\mathbf{1a}^-$ and $\mathbf{3aH}^+$, respectively, where the motifs of $\mathbf{1a}^-$ and $\mathbf{3aH}^+$ can be regarded as the left- and right-handed helices, respectively. Carbon atoms of $\mathbf{1a}^-$ and $\mathbf{3aH}^+$ were coloured by green and orange, respectively, while oxygen and nitrogen atoms by red and purple, respectively. All hydrogen atoms except for that in the salt bridge were omitted for clarity. Symmetry code: for (d) (*A*) 1/2 + *x*, 3/2 − *y*, −*z*; (*B*) −1/2 + *x*, 3/2 − *y*, −*z*; for (f) (*A*) −*x*, 1/2 + *y*, 1/2 − *z*; (*B*) −*x*, 1/2 + y, 1/2 − *z*.

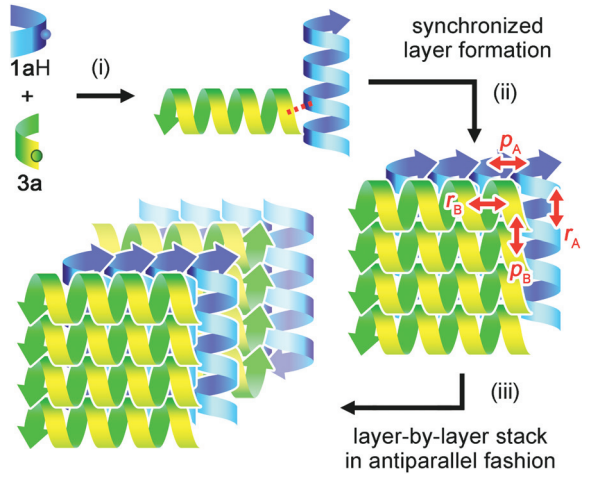

Fig. 9 Schematic representation for a hierarchical scenario to construct heteroH-MOC **1a·3a**H. The scenario contains the following processes: (i) formation of hetero helices by perpendicular connection of right- and left-handed helices through the salt bridge, (ii) synchronized layer formation, and (iii) lamination of the layer in an antiparallel fashion. The periodic synchronization: $r_A = p_B = 9.27$ Å and $r_B = p_A = 14.30$ Å.

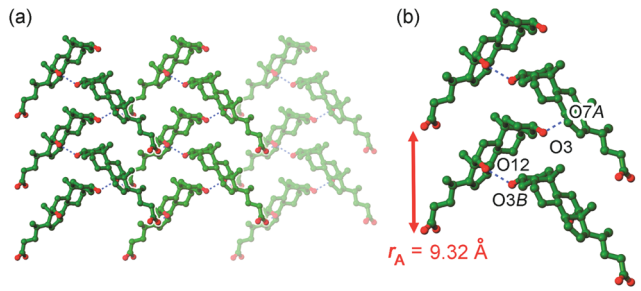

Fig. 10 (a) The sheet and (b) 2_1 helical motifs of **1b**$^-$ in the crystal **1b·3a**H. Carbon and oxygen atoms were coloured by green and red, respectively. All hydrogen atoms were omitted for clarity. Symmetry code: (d) (*A*) $1/2 + x$, $1/2 - y$, $1 - z$; (*B*) $-1/2 + x$, $1/2 - y$, $-z$.

3aH$^+$ to that from the O_{3a} to $N_{3a}2$ atoms in the O_{3a}–H···$N_{3a}2$ hydrogen bonds. A salt bridge was formed between **1a**$^-$ and **3a**H$^+$ (O′24···H–$N_{3a}1$ with O···N distance of 2.614 Å) as shown in Fig. 8b.

Construction of the heteroH-MOCs **1a·3a**H can be described by a hierarchical scenario as shown in Fig. 9, which experiences (i) formation of hetero helices by perpendicular connection of right- and left-handed helices through the salt bridge, (ii) synchronized layer formation, and (iii) lamination of the layer in an antiparallel fashion. In the crystal, synchronization between helical pitch and periodic distance of helices ($r_A = p_B = 9.27$ Å and $r_B = p_A = 14.30$ Å) was successfully achieved.

The same framework was also achieved with **1b·3a**H, in which **1b**$^-$ forms the similar sheet structure and 2_1 helical motif with those of **1a**$^-$, despite the hydroxyl group at the 7-position is lacked for **1b**H (Fig. 10). Conventionally, **1a**H and **1b**H gave completely different motifs in their inherent crystals. Namely, **1a**H forms typical multi-hydrogen-bonded 2_1 helical assemblies with pitch ranging 7.7–8.6 Å for $P2_1$ crystals[22] and 11.2–12.4 Å for $P2_12_12_1$ crystals.[23] Deoxycholic acid **1b**H, on the other hand, often forms layered motifs in $P2_12_12_1$ crystals, while hydrogen-bonded 2_1 helical assemblies with the pitch of *ca.* 7.2 Å are achieved only in a handful of crystals.[25] In the present system, their counter-component, **3a**H, forces the bile acids to form the same 2_1 helical motifs. Moreover, **1c**H and **1d**H, which are isomers of **1b**H, gave no crystal but an amorphous-film-like material and another type of crystals with $P2_1$ space group (*vide supra*). These results indicate that the hydroxyl group at the 12-position is necessary for formation of the herringbone typed 2_1 motif and that intra- and inter-columnar hydrogen bonds involving the 12-positioned hydroxyl group, that is, O12–H···O3 (see, Fig. 8d) and O24···H–O12 (see, Fig. 8a), respectively, stabilize the crystal structure.

Experimental

Single crystal diffraction data were collected on a Rigaku R-AXIS RAPID diffractometer with a 2-D area detector using graphite-monochromatized Cu Kα radiation ($\lambda = 1.54187$ Å) for **1a·3a**H, **1b·3a**H, **1e·3a**H, and **1e·3b**H, and by using the synchrotron radiation ($\lambda = 0.7000$ Å) for **1d·4a**H. The cell refinements of **1d·4a**H were performed with HKL2000 software.[24] Direct methods (SIR-2002 and 2004) were used for the structure solution of all crystals.[26] All calculations were performed with the observed reflections [$I > 2\sigma(I)$] with the program CrystalStructure crystallographic software packages, except for refinement, which was performed using SHELXL-97.[27] All non-hydrogen atoms were refined with anisotropic displacement parameters, except for 1,4-dioxane in **1e·3b**H, which are refined isotropically because of disorder. All hydrogen atoms were placed in idealized positions and refined as rigid atoms with the relative isotropic displacement parameters, except for those of the hydroxyl groups, whose positions were determined based on the residual electron density. The crystallographic parameters are listed in Table 2.

Conclusion

In this study, we proposed a new class of organic crystal, that is, heteroH-MOC (multi-component organic crystal containing different kinds of helical motifs consisted of different components). Screened cocrystallization with combination of five bile acids (**1a**H–**1e**H) and four cinchona alkaloids (**3a,b** and **4a, b**) successfully gave five heteroH-MOCs (**1a·3a**H, **1b·3a**H, **1e·3a**H, **1e·3b**H, and **1d·4a**H). These are the first examples for construction of heteroH-MOCs composed of 2_1 helices of cholic acid derivatives and cinchona alkaloids. In crystals **1e·3a**H, **1e·3b**H, and **1d·4a**H with $P2_1$ space group, two kinds of helices composed of the acid and base are arranged in a parallel fashion. On the other hand, $P2_12_12_1$ crystals **1a·3a**H and **1b·3a**H are established through perpendicular arrangements of the helices. In such systems, components ingeniously achieved highly-ordered synchronization of periodicity (helical pitches and periodic distances in the array of helices). Furthermore, in the present systems, one component obviously recognized molecular shapes and chirality of the counter-component through periodic synchronization. Therefore, heteroH-MOCs are appropriate systems

Table 2 Crystallographic parameters of the obtained crystals

Crystal	**1a·3a**H	**1b·3a**H	**1e·3a**H	**1e·3b**H	**1d·4a**H[a]
Formula	$(C_{24}H_{39}O_5)^-\cdot(C_{19}H_{23}N_2O)^+$	$(C_{24}H_{39}O_4)^-\cdot(C_{19}H_{23}N_2O)^+$	$(C_{24}H_{39}O_3)^-\cdot(C_{19}H_{23}N_2O)^+\cdot(C_4H_8O_2)_2\cdot(H_2O)_2$	$(C_{24}H_{39}O_3)^-\cdot(C_{20}H_{24}N_2O_2)^+\cdot(C_4H_8O_2)_2\cdot(H_2O)$	$(C_{24}H_{39}O_4)^-\cdot(C_{19}H_{23}N_2O)^+\cdot(C_4H_8O)_2\cdot(H_2O)$
Fw	702.97	686.97	883.20	895.21	849.19
Crystal system	Orthorhombic	Orthorhombic	Monoclinic	Monoclinic	Monoclinic
Space group	$P2_12_12_1$ (#19)	$P2_12_12_1$ (#19)	$P2_1$ (#4)	$P2_1$ (#4)	$P2_1$ (#4)
a [Å]	9.2659 (4)	9.3208 4)	11.4060(6)	11.2617 (5)	15.1052(2)
b [Å]	14.2973 (5)	14.1964 (6)	7.8884(4)	7.6842 (3)	6.53750(10)
c [Å]	29.1661 (11)	29.1726 (13)	27.0427(14)	27.7084 (12)	23.8816(4)
α [°]	90	90	90	90	90
β [°]	90	90	96.296(3)	93.487 (2)	95.8640(6)
γ [°]	90	90	90	90	90
V [Å^3]	3863.8 (2)	3860.2 (3)	2418.5(2)	2393.36 (18)	2345.97(6)
Z	4	4	2	2	2
Dc [g cm^{-3}]	1.208	1.182	1.213	1.242	1.202
Uni./obs.	7031/36 701	6961/36 746	8146/24 406	7356/23 896	6941/34 216
Ref.					
R_1/Rw	0.0862/0.1872	0.0613/0.1779	0.0865/0.2553	0.1664/0.4750	0.1076/0.3477
T [°C]	−60	−60	−60	−60	−180

[a] The crystallographic refinement for **1d·4a**H was not sufficient because of limitation of crystallographic analysis.

for understanding the chiral discrimination mechanism and can be applied practically.

Acknowledgements

This work was supported by KAKENHI (21245035, 22108517, 22651042) from MEXT (Japan). T.S. thanks the Global COE (center of excellence) Program "Global Education and Research Center for Bio-Environmental Chemistry" of Osaka University for financial support. We are grateful to Dr K. Miura, Dr S. Baba, and Dr N. Mizuno for crystallographic data collection at the BL38B1 in the SPring-8 with the approval of JASRI (proposal No. 2007B2039, 2007B2005, 2007B1988, 2008A1422, 2009B1969 and 2011B1587).

Notes and references

1 (*a*) E. Yashima, K. Maeda, H. Iida, Y. Furusho and K. Nagai, *Chem. Rev.*, 2009, **109**, 6102; (*b*) J. Kumaki, S. Sakuraiya and E. Yashima, *Chem. Soc. Rev.*, 2009, **38**, 737.
2 K. Akagi, *Chem. Rev.*, 2009, **109**, 5354.
3 D. J. Hill, M. J. Mio, R. B. Prince, T. S. Hughes and J. S. Moore, *Chem. Rev.*, 2001, **101**, 3893.
4 (*a*) C. Piguet, G. Bernardinelli and G. Hopfgartner, *Chem. Rev.*, 1997, **97**, 2005; (*b*) M. Albrecht, *Chem. Rev.*, 2001, **101**, 3457.
5 T. Shimizu, M. Masuda and H. Minamikawa, *Chem. Rev.*, 2005, **105**, 1401.
6 (*a*) J. Kumaki, T. Kawauchi, K. Okoshi, H. Kusanagi and E. Yashima, *Angew. Chem., Int. Ed.*, 2007, **46**, 5348; (*b*) S. Sakurai, S. Ohsawa, K. Nagai, K. Okoshi, J. Kumaki and E. Yashima, *Angew. Chem., Int. Ed.*, 2007, **46**, 7605; (*c*) S. Sakurai, K. Okoshi, J. Kumaki and E. Yashima, *J. Am. Chem. Soc.*, 2006, **128**, 5650.
7 (*a*) K. Sugikawa, M. Numata, D. Kinoshita, K. Kaneko, K. Sada, A. Asano, S. Seki and S. Shinkai, *Org. Biomol. Chem.*, 2011, **9**, 146; (*b*) M. Numata and S. Shinkai, *Chem. Commun.*, 2011, **47**, 1961.
8 A. I. Kitaigorodskii, *Molecular Crystals and Molecules*, Academic Press, London, 1973.
9 http://www.ccdc.cam.ac.uk/products/csd/
10 (*a*) F. H. Herbstein, in *Crystalline Molecular Complexes and Compounds*, Oxford University Press, New York, 2005, vol. 1, p. 2; (*b*) C. B. Aakeröy and N. Schultheiss, in *Making Crystals by Design*, ed. D. Braga and F. Grepioni, Wiley-VCH, Weinheim, 2007, pp. 209–240.
11 For example, see: (*a*) C. B. Aakeröy and D. J. Salmon, *CrystEngComm*, 2005, **7**, 439; (*b*) R. Banerjee, P. M. Bhatt, N. V. Ravindra and G. R. Desiraju, *Cryst. Growth Des.*, 2005, **5**, 2299; (*c*) N. J. Babu, L. S. Reddy, S. Aitipamula and A. Nangia, *Chem.–Asian J.*, 2008, **3**, 1122.
12 (*a*) H. Koshima, M. Kamada, I. Yagi and K. Uosaki, *Cryst. Growth Des.*, 2001, **1**, 467; (*b*) M. J. Prakash and T. P. Radhakrishnan, *Cryst. Growth Des.*, 2005, **5**, 721.
13 (*a*) K. Kodama, Y. Kobayashi and K. Saigo, *Chem.–Eur. J.*, 2007, **13**, 2144; (*b*) Y. Imai, K. Kawaguchi, N. Tajima, T. Sato, R. Kuroda and Y. Matsubara, *Chem. Commun.*, 2008, 362.
14 (*a*) A. Matsumoto, S. Nagahama and T. Odani, *J. Am. Chem. Soc.*, 2000, **122**, 9109; (*b*) A. Matsumoto, T. Tanaka, T. Tsubouchi, K. Tashiro, S. Saragai and S. Nakamoto, *J. Am. Chem. Soc.*, 2002, **124**, 8891; (*c*) A. Matsumoto, K. Sada, K. Tashiro, M. Miyata, T. Tsubouchi, T. Tanaka, T. Odani, S. Nagahama, T. Tanaka, K. Inoue, S. Saragai and S. Nakamoto, *Angew. Chem., Int. Ed.*, 2002, **41**, 2502; (*d*) S. Nagahama, K. Inoue, K. Sada, M. Miyata and A. Matsumoto, *Cryst. Growth Des.*, 2003, **3**, 247; (*e*) K. Sada, K. Inoue, T. Tanaka, A. Tanaka, A. Epergyes, S. Nagahama, A. Matsumoto and M. Miyata, *J. Am. Chem. Soc.*, 2004, **126**, 1764.
15 I. Hisaki, N. Shizuki, K. Aburaya, M. Katsuta, N. Tohnai and M. Miyata, *Cryst. Growth Des.*, 2009, **9**, 1280.
16 Examples of hierarchical interpretation for crystals, see: (*a*) A. Tanaka, K. Inoue, I. Hisaki, N. Tohnai, M. Miyata and A. Matsumoto, *Angew. Chem., Int. Ed.*, 2006, **45**, 4142; (*b*) M. Miyata, N. Tohnai and I. Hisaki,

Acc. Chem. Res., 2007, **40**, 694; (*c*) I. Hisaki, H. Senga, H. Shigemitsu, N. Tohnai and M. Miyata, *Chem.–Eur. J.*, 2011, **17**, 14348; (*d*) I. Hisaki, E. Kometani, H. Shigemitsu, N. Tohnai and M. Miyata, *Cryst. Growth Des.*, 2011, **11**, 5488.

17 (*a*) S. K. Arora, G. Germain and J. P. Declercq, *Acta Crystallogr., Sect. B: Struct. Crystallogr. Cryst. Chem.*, 1976, **32**, 415; (*b*) E. Virtanen, M. Nissinen, R. Suontamo, J. Tamminen and E. Kolehmainen, *J. Mol. Struct.*, 2003, **649**, 207.

18 (*a*) I. Hisaki, N. Tohnai and M. Miyata, *Chirality*, 2008, **20**, 330.

19 (*a*) A. Tanaka, I. Hisaki, N. Tohnai and M. Miyata, *Chem.–Asian J.*, 2007, **2**, 230; (*b*) T. Yuge, T. Sakai, N. Kai, I. Hisaki, M. Miyata and N. Tohnai, *Chem.–Eur. J.*, 2008, **14**, 2984; (*c*) I. Hisaki, N. Shizuki, T. Sasaki, Y. Ito, N. Tohnai and M. Miyata, *Cryst. Growth Des.*, 2010, **10**, 5262; (*d*) T. Watabe, K. Kobayashi, I. Hisaki, N. Tohnai and M. Miyata, *Bull. Chem. Soc. Jpn.*, 2007, **80**, 464; (*e*) I. Hisaki, T. Sasaki, K. Sakaguchi, W.-T. Liu, N. Tohnai and M. Miyata, *Chem. Commun.*, 2012, **48**, 2219.

20 (*a*) S. R. Hall, E. N. Maslen and A. Cooper, *Acta Crystallogr., Sect. B: Struct. Crystallogr. Cryst. Chem.*, 1974, **30**, 1441; (*b*) K. Nakano, Y. Hishikawa, K. Sada, M. Miyata and K. Hanabusa, *Chem. Lett.*, 2000, **29**, 1170.

21 For example, see: (*a*) R. Doherty, W. R. Benson, M. Maienthal and J. McD. Stewart, *J. Pharm. Sci.*, 1978, **67**, 1698; (*b*) H. Ohbo, H. Okazaki, K. Miyoshi and H. Yoneda, *Bull. Chem. Soc. Jpn.*, 1983, **56**, 1982; (*c*) S. Larsen, H. L. de Diego and D. Kozma, *Acta Crystallogr., Sect. B: Struct. Sci.*, 1993, **49**, 310; (*d*) J. Lacour, C. Ginglinger, C. Grivet and G. Bernardinelli, *Angew. Chem., Int. Ed. Engl.*, 1997, **36**, 608; (*e*) B. Dominguez, A. Zanotti-Gerosa and W. Hems, *Org. Lett.*, 2004, **6**, 1927; (*f*) P. M. Bhatt, N. V. Ravindra, R. Banerjee and G. R. Desiraju, *Chem. Commun.*, 2005, 1073.

22 $P2_1$ crystals, see for example: (*a*) K. Miki, A. Masui, N. Kasai, M. Miyata, M. Shibakami and K. Takemoto, *J. Am. Chem. Soc.*, 1988, **110**, 6594; (*b*) M. R. Caira, L. R. Nassimbeni and J. L. Scott, *Chem. Commun.*, 1993, 612; (*c*) M. Shibakami, M. Tamura and A. Sekiya, *J. Am. Chem. Soc.*, 1995, **117**, 4499; (*d*) M. Gdaniec and T. Połoński, *J. Am. Chem. Soc.*, 1998, **120**, 7353; (*e*) M. Gdaniec, M. J. Milewska and T. Połoński, *Angew. Chem., Int. Ed.*, 1999, **38**, 392; (*f*) K. Nakano, K. Sada, Y. Kurozumi and M. Miyata, *Chem.–Eur. J.*, 2001, **7**, 209; (*g*) K. Nakano, E. Mochizuki, N. Yasui, K. Morioka, Y. Yamauchi, N. Kanehisa, Y. Kai, N. Yoswathananont, N. Tohnai, K. Sada and M. Miyata, *Eur. J. Org. Chem.*, 2003, 2428; (*h*) K. Nakano, K. Sada, K. Aburaya, K. Nakagawa, N. Yoswathananont, N. Tohnai and M. Miyata, *CrystEngComm*, 2006, **8**, 461.

23 $P2_12_12_1$ crystals, see for example: (*a*) P. L. Johnson and J. P. Schaefer, *Acta Crystallogr., Sect. B: Struct. Crystallogr. Cryst. Chem.*, 1972, **28**, 3083; (*b*) E. L. Jones and L. R. Nassimbeni, *Acta Crystallogr., Sect. B: Struct. Sci.*, 1990, **46**, 399; (*c*) M. Miyata, M. Shibakami, S. Chirachanchai, K. Takemoto, N. Kasai and K. Miki, *Nature*, 1990, **343**, 446; (*d*) K. Miki, N. Kasai, M. Shibakami, S. Chirachanchai, K. Takemoto and M. Miyata, *Acta Crystallogr., Sect. C: Cryst. Struct. Commun.*, 1990, **46**, 2442; (*e*) M. Shibakami and A. Sekiya, *J. Inclusion Phenom. Macrocyclic Chem.*, 1994, **18**, 39; (*f*) K. Nakano, K. Sada and M. Miyata, *Chem. Commun.*, 1996, 989; (*g*) N. Yoswathananont, S. Chirachanchai, K. Tashiro, K. Nakano, K. Sada and M. Miyata, *CrystEngComm*, 2001, **3**, 74.

24 K. Sada, N. Shiomi and M. Miyata, *J. Am. Chem. Soc.*, 1998, **120**, 10543.

25 Z. Otwinowski and W. Minor, *Methods Enzymol.*, 1997, **276**, 307.

26 A. Altomare, M. Burla, M. Camalli, G. Cascarano, C. Giacovazzo, A. Guagliardi, A. Moliterni, G. Polidori and R. Spagna, *J. Appl. Crystallogr.*, 1999, **32**, 115.

27 G. M. Sheldrick, *Acta Crystallogr., Sect. A: Found. Crystallogr.*, 2008, **64**, 112.

